

AMP Methods for Fourier-Structured Operators and Signals

Saurav K. Shastri, Rizwan Ahmad,
Christopher A. Metzler, Philip Schniter



2022 Asilomar Conf. on Signals, Systems, and Computers
Paper ID: 1261
Supported in part by NSF CCF-1955587 and NIH R01-EB029957

Plug-and-Play (PnP) image recovery

- Goal: Recover an unknown image x_0 from noisy parallel MRI measurements y

$$y = \underbrace{\begin{bmatrix} MF \text{Diag}(s_1) \\ \vdots \\ MF \text{Diag}(s_C) \end{bmatrix}}_{\triangleq A} x_0 + w, \text{ with } \begin{cases} M: \text{ sampling mask} \\ F: \text{ 2D Fourier transform} \\ s_c: \text{ estimated coil map} \end{cases}$$

- Plug-and-play (PnP) algorithms iteratively call a deep-net image denoiser, which can be trained ...

- from very few images, using patches
- independently of A , facilitating generalization to any A

- But there are some downsides to PnP:

- PnP algs require careful tuning of parameters and early stopping
- The denoiser input-error is non-white and non-Gaussian, and difficult to characterize, so it's unclear how to optimally train the denoiser

Approximate message passing (AMP) algorithms

- AMP is a family of autotuning PnP algorithms that have remarkable properties for large random A :

- The denoiser input-error is AWGN with predictable variance
- With an MMSE denoiser, AMP algs converge to the MMSE estimate of x_0 given y

- Challenge: In most signal recovery problems, A does not satisfy AMP's randomness assumptions!

AMP for parallel magnetic resonance (MR) imaging

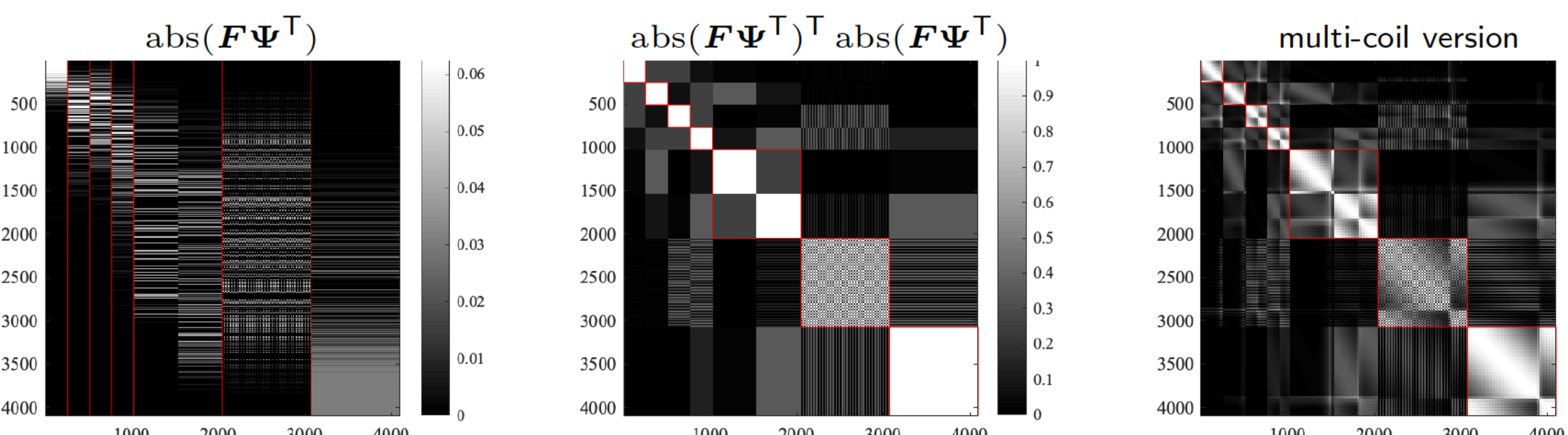
- For parallel MRI, damped AMP has been proposed [Sarkar et al'21]
 - but it is heuristic and doesn't appear to follow a state evolution

- For MRI with 2D point masks, modified VAMP algs were proposed: VDAMP [Millard et al'20] and P-VDAMP [Millard et al'22]
 - but 2D point masks are impractical and uncommon in 2D MRI

- Proposed approach: Recover the wavelet coefficients c_0 , not pixels x_0 .
 - This gives $y = Bc_0 + w$ with masked Fourier-wavelet matrix $B = A\Psi^T$

- For AMP algorithms, B has desirable behavior:

- columns of different subbands are relatively decoupled from each other
- columns of each subband have a randomizing effect on that subband



Proposed algorithm: Denoising GEC (D-GEC)

We build upon the generalized expectation consistent (GEC) algorithm from Fletcher et al'16:

```

require:  $f_1(\cdot)$ ,  $f_2(\cdot)$ , and  $\text{gdiag}(\cdot)$ 
initialize:  $r_1, \gamma_1$ 
for  $t = 0, 1, 2, \dots$ 
     $\hat{x}_1 \leftarrow f_1(r_1, \gamma_1)$  linear estimation
     $\eta_1 \leftarrow \text{Diag}(\text{gdiag}(\nabla f_1(r_1, \gamma_1)))^{-1} \gamma_1$ 
     $\gamma_2 \leftarrow \eta_1 - \gamma_1$ 
     $r_2 \leftarrow \text{Diag}(\gamma_2)^{-1} (\text{Diag}(\eta_1) \hat{x}_1 - \text{Diag}(\gamma_1) r_1)$  Onsager

     $\hat{x}_2 \leftarrow f_2(r_2, \gamma_2)$  denoising
     $\eta_2 \leftarrow \text{Diag}(\text{gdiag}(\nabla f_2(r_2, \gamma_2)))^{-1} \gamma_2$ 
     $\gamma_1 \leftarrow \eta_2 - \gamma_2$ 
     $r_1 \leftarrow \text{Diag}(\gamma_1)^{-1} (\text{Diag}(\eta_2) \hat{x}_2 - \text{Diag}(\gamma_2) r_2)$  Onsager
    
```

- GEC is essentially Peaceman-Rachford ADMM with adaptive vector-valued stepsizes γ_1 and γ_2

- The GEC linear estimation stage is preconditioned LS:

$$f_1(r, \gamma) = (\gamma_w B^H B + \text{Diag}(\gamma))^{-1} (\gamma_w B^H y + \text{Diag}(\gamma) r)$$

which can be implemented using the conjugate gradient method

- For f_2 , we propose to "plug in" a deep denoiser

- ∇f_i denotes the Jacobian, and $\text{gdiag}(\cdot)$ averages its diagonal across different wavelet subbands. D-GEC approximates the Jacobian using a Monte-Carlo approach [Ramani et al'08]

Proposed denoiser: Corr+Corr

- GEC yields denoiser input-error that is AWGN with known iteration- and subband-dependent precisions γ in each wavelet subband

- In the pixel domain, the error is correlated Gaussian with known covariance matrix $\Psi \text{Diag}(\gamma)^{-1} \Psi^T$
 - How should we inform the denoiser about (Ψ, γ) ?

- We take an arbitrary existing denoiser (e.g., DnCNN) and feed independent realizations of $\mathcal{N}(0, \Psi \text{Diag}(\gamma)^{-1} \Psi^T)$ into extra channels
 - The denoiser learns to extract the error statistics
 - We call it "corr+corr"

- Example PSNRs for depth-1 2D wavelet transform:

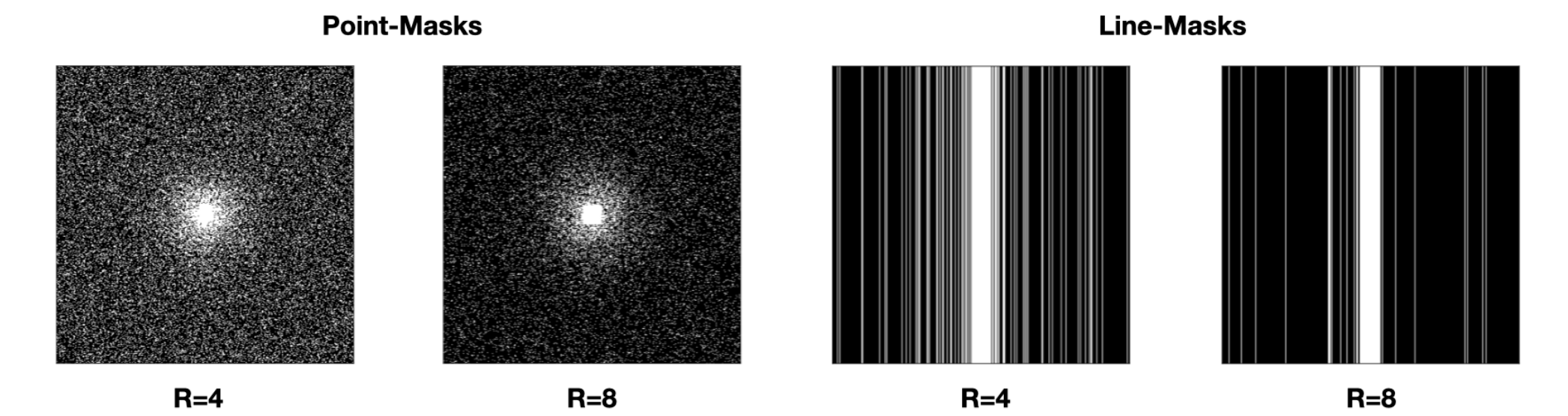
$\sqrt{\gamma^{-1}}$	white DnCNN	Metzler et al'21 DnCNN	corr+corr DnCNN	genie DnCNN
[48,47,6,19]	25.36	31.23	31.69	32.12
[10,40,23,14]	32.44	34.87	35.24	35.54
[13,7,8,10]	36.50	31.03	37.02	37.41
[10,10,10,10]	37.41	31.94	37.31	37.63
uniform [0-50,0-50,0-50,0-50]	31.07	33.24	34.08	—

white DnCNN trained unif [0-50]; Metzler et al'21 DnCNN & corr+corr DnCNN trained unif [0-50,0-50,0-50,0-50]

MR image recovery experiments

- Setup:

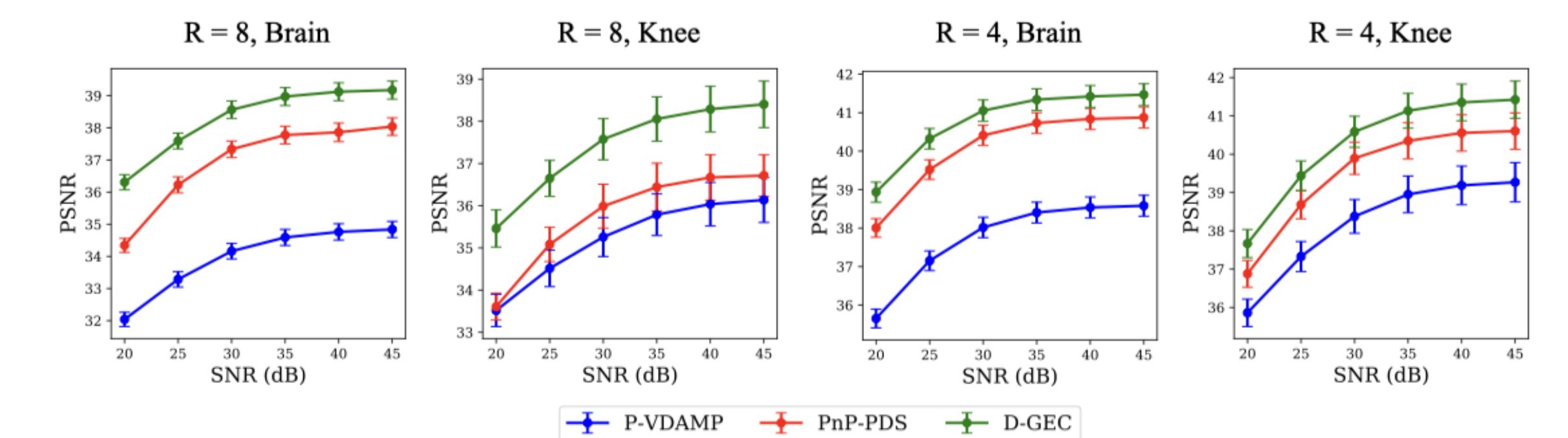
- multi-coil fastMRI [Zbontar et al'18] brain and knee data
- 8 virtual coils; acceleration $R = N/M = 4 \& 8$
- additional AWGN w for noise-robustness study
- variable-density 2D point- and line-masks:



- 2D line-mask results averaged over 16 test images:

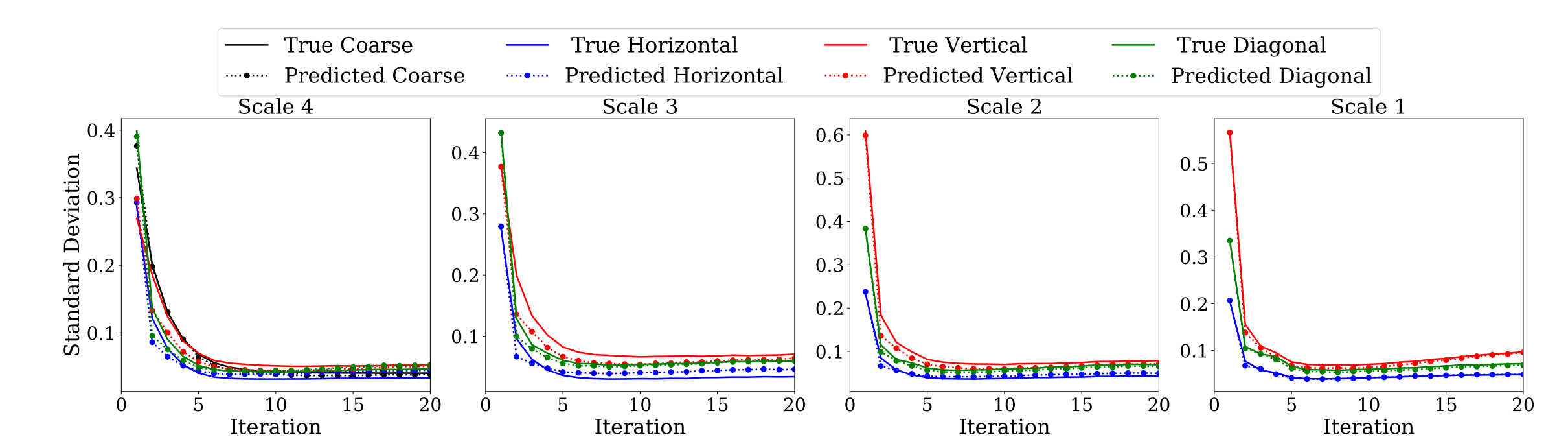
method	Knee				Brain			
	R=4		R=8		R=4		R=8	
	PSNR	SSIM	PSNR	SSIM	PSNR	SSIM	PSNR	SSIM
P-VDAMP	33.84	0.9018	20.34	0.5614	30.30	0.8847	13.51	0.4763
PnP-PDS	36.28	0.9204	32.34	0.8556	38.07	0.9501	28.97	0.8269
D-GEC	38.82	0.9504	33.66	0.8893	39.04	0.9631	30.61	0.9015

- Average PSNR versus measurement SNR with 2D point-mask:

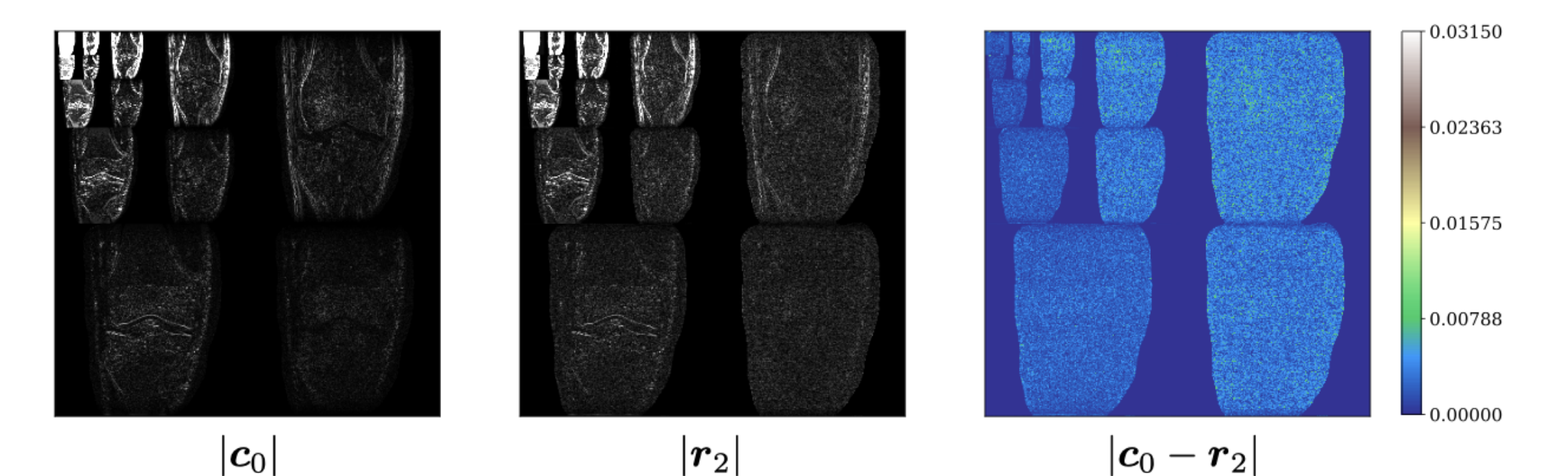


Note: PnP-PDS penalty and stopping iteration tuned for every (SNR, R, dataset)

- Predictability of D-GEC error variance vs iteration with 2D line-mask at R=4:



- Example wavelet error at iteration 10 with 2D line-mask at R=4:



- Example wavelet-error QQ plots at iteration 10 with 2D line-mask at R=4:

